Catalytic Activity in CO Oxidation of MnO_x Supported on Oxides and Zeolites

Larisa V. Lutsenko[a*], Ludmila P. Oleksenko[a], German M. Telbiz[b], Victoriia G. Gerasova[a]

[a] *Department of Chemistry, Taras Shevchenko National University of Kyiv, Volodymyrska Street, 64/13, Kyiv 01601, Ukraine*

[b] *Institute of Physical Chemistry, NAS of Ukraine, 31 Nauki av., Kyiv, 03028, Ukraine*

larisa_lutsenko@ukr.net

Keywords: *MnO_x, CO oxidation, TPR, IR of adsorbed CO, DR UV–Vis.*

Catalytic activity in CO oxidation was investigated for MnO_x-containing materials, prepared by impregnation of SiO_2, Al_2O_3 and zeolites (ZSM-5, ERI). The catalysts were characterized by temperature-programmed reduction (TPR) by hydrogen, diffuse-reflectance UV–Vis (DR UV–Vis) and infra-red (IR) spectroscopy of adsorbed CO. Effect of the previous treatment of the MnO_x-containing systems on the catalytic performance has been established. Higher catalytic activity in CO oxidation of the materials treated with air as compared with treated with hydrogen can be explained by presences of manganese ions in +3 and +4 oxidation states. 3%Mn-SiO_2 previously treated with air at 350 °C is found to be the most active catalyst among the studied ones.

Introduction

Nowadays, metal oxides are proposed as interesting alternatives for more expensive noble metals in a variety of catalytic oxidation processes of industrial significance. It is known, that manganese oxide containing systems were reported to show catalytic efficiency for NO_x removal [1–3], CO oxidation [4–7], volatile organic compound abatement [6–9], removing of which from industrial wastes are extremely important for respiratory and environmental protection.

For stoichiometric manganese oxides orders of catalytic activities for CO oxidation are somewhat controversy: some researchers present $MnO \leq MnO_2 < Mn_2O_3$ activity order (at 523 K) [10–11], but other researches reports MnO_2 as the most active oxide [12–13]. Their activity is explained to the ease of changing of manganese oxidation state. Structural flexibility of manganese oxides, which exist in a number of different stoichiometric and non-stoichiometric phases, where Mn oxidation state varies from +2 (in MnO) to +4 (in MnO_2), can cause low-temperature CO oxidation activity [6–8]. As result unsupported and supported mixed manganese oxides show good catalytic properties too.

Actually, variation of the catalytic activity for different manganese oxides can be explained from the morphology viewpoint, by assuming that specific surface termination and

Mn–O bond strengths are the determining factors [10]. Hence, catalytic performance is largely influenced by the nature, particularly the oxidation state, of supported manganese species. In turn oxidation state of the manganese species is strongly affected by the preparation conditions, such as metal precursor, metal loading, thermal treatment conditions (temperature, oxidative or reductive atmosphere) [14]. Suport plays a noticeable role too. It is known that inert character of silica promotes formation of interface, in which metal oxide species are not strongly associated with silica surface, and active sites are easily reduced at low temperature, what is favorable for catalytic performance in oxidation reactions [15]. Alumina is a typical support for noble metal containing catalysts in industry and is also interesting to study as support in noble metal-free systems [16]. Also, zeolites are perspective supports due to their structural properties promoting good distribution of active metal species [17], and there are few reports concerning manganese-zeolite systems in CO oxidation.

In this paper MnO_x-containing catalysts supported on SiO_2, Al_2O_3 and zeolites were obtained and their redox, adsorption properties and the activity in CO oxidation depending on previous treatment conditions are studied. As zeolite supports ZSM-5 (Si/Al = 18.5; channels: 0.54 x 0.56, 0.51 x 0.55) and erionite (ERI) (Si/Al = 3.6; channels: 0.36 x 0.52) [18] were used. Alpha-alumina modification is used, it has high thermal, mechanical and chemical stability, few studied in CO oxidation, and differs by morphological features from other supports of the study greater than more widely used γ-Al_2O_3 (larger pore diameters, less specific surface area) [19].

Experimental

Manganese containing systems were obtained by impregnation of supports with $Mn(NO_3)_2$ solution. These samples were dried at the ambient pressure overnight at 60 °C. As supports SiO_2 (Silochrom S-120), α-Al_2O_3 (“pure for analysis” mark), zeolites ZSM-5 and ERI (“Nizhnegorodskie sorbenty”, Russia) were used.

The samples on the base of ZSM-5 with various metal loading – 1, 1.5, 2, 2.5, 3, 3.5 and 4 wt.% Mn – were prepared and used in catalytic reaction. The catalysts containing 3% wt.% Mn on oxide and zeolite supports (denoted as Mn-SiO_2, Mn-Al_2O_3, Mn-ERI and Mn-ZSM-5) were prepared and used in catalytic reaction after previous treatment with: a) H_2 (10%H_2+90%Ar mixture was used) during 1 h at temperature 350 °C; b) air during 1 h at temperature 350 °C; c) air during 1 h at temperature 500 °C.

Catalytic measurements of manganese containing systems in CO oxidation were carried out in a flow reactor with chromatographic control of reaction mixture

composition using thermal conductivity detector TCD. The catalytic activity was investigated under atmosphere pressure in the range 20 – 350 ºC (from 20 °C to the temperature when CO conversed to CO_2 completely) in reaction mixture 1% CO + 20% O_2 + 79% He. The temperature of total CO conversion (T_{100}) was a measure of catalytic activity.

To carry out temperature programmed reduction by hydrogen, the samples were merged in a quartz reactor, heated in Ar at 350 °C, and spectra were registered using heating of samples from room temperature to 800 ºC with increment 10 °C/min under a gas flow 10%H_2+90%Ar. The hydrogen consumption was monitored with TCD.

IR study of adsorbed CO was performed on self-supported wafers (0.06-0.08 g) using a Specord IR-75 (“Carl Zeiss”) spectrometer. The wafer was fixed with a molybdenum steel holder located in a sample holder of a quartz cell with KBr windows, which were cooled by water circulating through blocks in thermal contact with the windows. The samples were first activated in a vacuum (at room temperature and P < 1.33 Pa) and further at 450 ºC in a vacuum during 30 min. A high-purity CO was used as CO source that was exposed in a cell at room temperature up to 20 h. Infrared spectra of the samples were obtained at 2 cm^{-1} resolution at room temperature after removing of physically adsorbed CO.

Diffuse-reflectance UV–Vis spectroscopy studies were carried out with spectrophotometer “Specord M-40", spectra were collected in the 250–800 nm wave-length range. For all spectra Kubelka-Munk function was calculated.

Specific surface areas of initial supports and 3%Mn-systems were measured by argon heat desorption method chromatografically using TCD. Activated at 200 °C with Ar to remove adsorbed substances sample in a reactor was passed by 20%Ar+80%He gas flow. The reactor was merged in liquid nitrogen for argon adsorption, and after attaining equilibrium and adsorption peak registration the reactor was merged in room temperature (water) for obtaining of argon desorption peak. Surface area was calculated by comparison of desorption peak referred to mass for a studied sample with standard sample of known surface area.

The total pore volume *V* was evaluated by water vapor at $p/p_s = 0.1$.

Results and discussion

Earlier it was shown that ZSM-5 zeolite is a perspective support for active metal-containing catalysts of CO oxidation [20]. Therefore catalytic activity in CO oxidation of Mn-containing systems depending on manganese loading (1–4 wt.% Mn) was tested at using ZSM-5 as support. It is found that dependence for total conversion of CO on

manganese loading has an extreme for 3%Mn-ZSM-5 sample **(Figure 1)**.

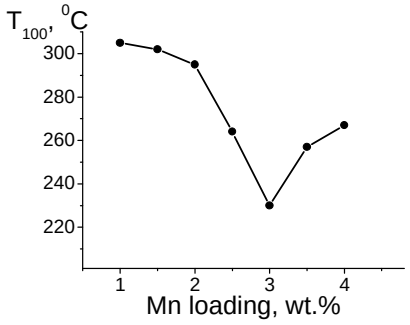

Figure 1. The dependence of T_{100} on manganese loading for 1–4 wt.% Mn-ZSM-5.

Thereby this optimal loading of manganese (3 wt.%) was applied to study an influence of previous treatment of the Mn-catalysts supported on oxides and zeolites on their activity. Catalytic measurements show that using of hydrogen thermal treatment at 350 ºC results in following activity order (**Table 1**): Mn-SiO_2 > Mn-Al_2O_3 > Mn-ZSM-5 > Mn-ERI.

Table 1. Temperatures of total CO conversion of the catalysts

Sample	T_{100}, °C		
	H_2, 350 °C	Air, 350 °C	Air, 500 °C
Mn-SiO_2	275	200	250
Mn-Al_2O_3	295	270	234
Mn-ZSM-5	302	274	224
Mn-ERI	326	286	257

It is known that active centers of a different nature can arise in a surface layer of the catalysts during treatment of them by H_2 and following development in the reaction gaseous mixture [21–22]. A support nature may determine an interaction degree of active sites with support surface and cause a various reducibility of entrapped manganese ions and therefore effect on the formation of different active sites.

To investigate the activity of oxide catalysts containing manganese ions in higher oxidation states an oxidative thermal treatment in air was employed for 3%Mn-systems. As shown in **Table 1**, all the catalysts previously treated with air reveal higher activity than ones treated with hydrogen. Most significant improvement is fixed in the case of Mn-SiO_2 (ΔT = 75 °C). The activity order of the manganese containing catalysts treated with air at 350°C is proved to be the same as the activity order observed for the catalysts with hydrogen treatment: Mn-SiO_2 > Mn-Al_2O_3 > Mn-ZSM-5 > Mn-ERI (**Table 1**).

The distinctions between catalytic activities of Mn-systems supported on oxides after reductive and oxidative previous treatments may be caused by different nature of sites participating in the catalytic reaction and ability for manganese based catalysts to stabilize simultaneously several oxide phases with different average oxidation states.

The TPR profiles of Mn-systems previously treated with air at 350 ºC, presented in **Figure 2**, contain some peaks of hydrogen consumption in the temperature range 180 – 475

ºC for all the systems, suggesting a multiple-step reduction process.

MnO_2 and Mn_2O_3 species are known to arise from manganese nitrate decomposition [23–24]. At introducing of small amount of the precursor (a few weight percents of manganese) into support a noticeable amount of Mn^{2+} is also formed because support is known can an effect on stabilization of low-valence manganese oxide species [25]. The low-temperature reduction peaks (LTRP) (180–350 °C) are assigned to reduction of MnO_2 and Mn_2O_3 species, in accordance with that the highest oxides have lower onset temperatures of reduction. At temperatures above 350 ºC a reduction of Mn^{2+} ions more strongly interacting with support and so haven't high reducibility, happens. It should be noted, that the direct assignment of peaks on the TPR profiles is rather difficult because of occurring non-stoichiometric MnO_x species at the process of reduction of manganese, entrapped in oxide system. Consequently, the composition, structure and surface properties of MnO_x-containing systems should be waited easily to change depending on catalyst preparation way and thermal conditions of reduction treatment [25].

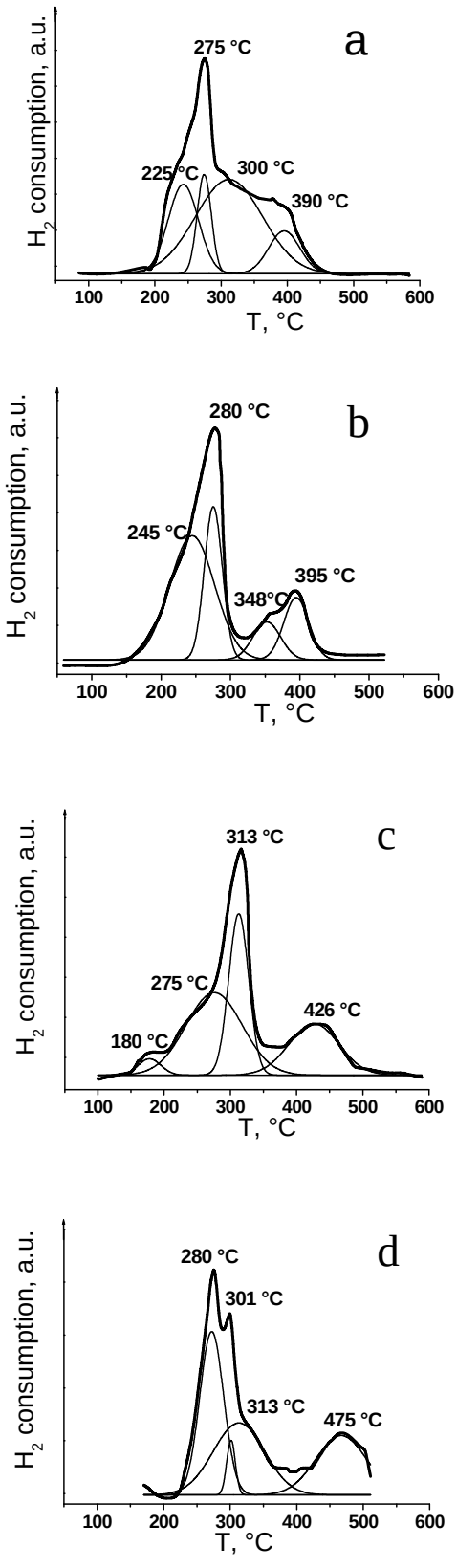

Figure 2. The TPR profiles of 3%Mn-systems treated with air at 350 ºC: a) Mn-SiO_2; b) Mn-Al_2O_3; c) Mn-ZSM-5; d) Mn-ERI.

The observed on TPR-profile lower H_2 consumption in high-temperature reduction peak (HTRP) region (350–500 °C) as compared with consumption in LTRP region (**Figure 2**) is likely to point at incomplete reduction of oxide species consisting Mn^{4+} and Mn^{3+} ions to Mn^{2+}. The presence of light brown and grey granules in the samples after TPR investigation also testifies to that.

The examination of reducibility of 3%Mn-containing catalysts and evaluation of the relative amount of manganese oxide forms, estimated by areas of the corresponding peaks on the TPR-profiles (**Figure 2**), shows that the greater amount of Mn ions of the highest reducibility (greater hydrogen consumption of LTRP) in Mn-catalyst, the higher its catalytic activity. In the case of the most active sample Mn-SiO_2 the relative amount of LTRP is the greatest and is equal to 88.7%. Lesser relative amounts of the LTRP for catalysts Mn-Al_2O_3 (85.8%), Mn-ZSM-5 (76.2%) and Mn-ERI (72.9%) as compared with Mn-SiO_2 correspond to slightly lower activities. Due to the TPR-H_2 it is shown that the relative amount of the easily-reduced manganese ions and the ratio LTRP to HTRP correspond to the increase in catalytic activity of the investigated samples.

The IR-spectra of CO adsorbed on 3%Mn-systems treated with air at 350 °C are presented in **Figure 3**. Adsorption of CO on Mn-catalysts supported on ZSM-5, SiO_2 and Al_2O_3 results in appearance of two bands with maxima at 2106 – 2118 cm^{-1} and 2154 – 2160 cm^{-1} (**Figure 3, curves 1-3**). According to [7, 26–27] these bands can be assigned to carbonyls Mn^{2+}–CO, apparently corresponding to $\nu_{as}(CO)$ and $\nu_s(CO)$ respectively [26]. In the spectrum of CO adsorbed on Mn-ERI (**Figure 3, curve 4**) one wide band at lower frequency (2004 cm^{-1}) is observed and it can be assigned to carbonate-carboxylate structures [14]. Reluctant formation of complexes of CO with manganese ions is in the agreement with the lowest catalytic activity of the Mn-ERI. It is worth noticing that all the carbonyls formed at 3%Mn-systems are unstable and the corresponding bands disappear from the spectra upon evacuation of CO at room temperature.

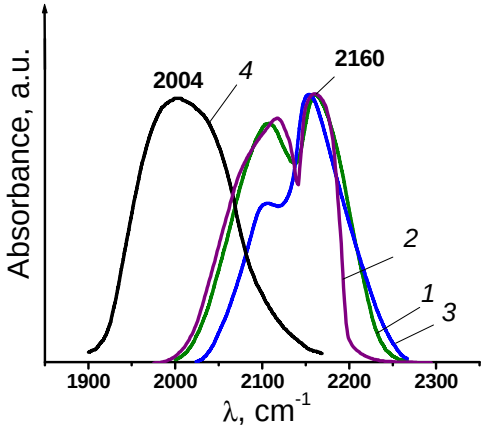

Figure 3. The IR-spectra of adsorbed CO on 3%Mn-systems treated with air at 350 ºC): 1) Mn-SiO_2; 2) Mn-Al_2O_3; 3) Mn-ZSM-5; 4) Mn-ERI.

Normalized DR UV–Vis spectra with Kubelka-Munk conversion for 3%Mn-systems treated with air at 350 ºC before and after catalytic reaction of CO oxidation (denoted

hereafter as initial and used samples, respectively) are shown in **Figure 4, a**.

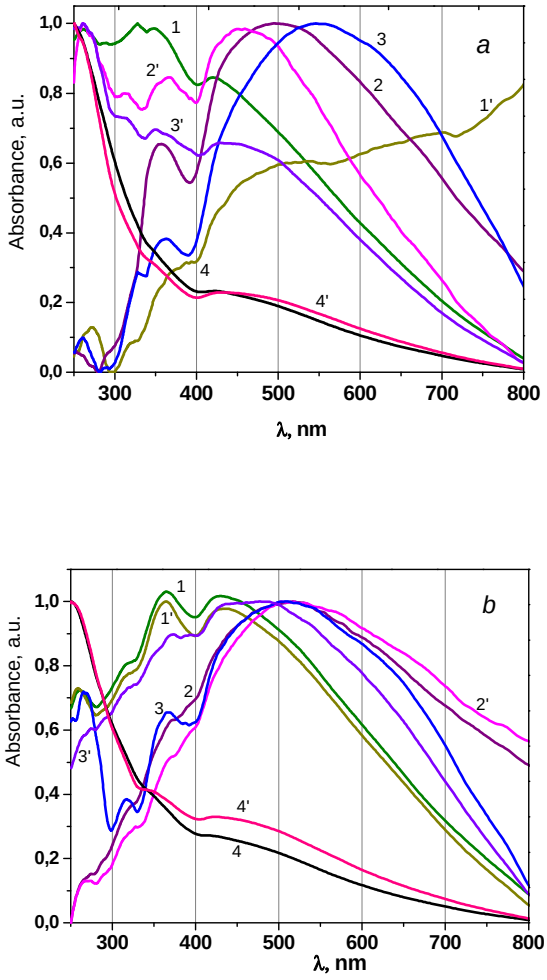

Figure 3. The DR UV–Vis spectra of 3%Mn-systems treated with air at 350 ºC (a); 500 °C (b): 1,1'– Mn-SiO_2; 2,2'– Mn-Al_2O_3; 3,3'– Mn-ZSM-5; 4,4'– Mn-ERI (1-4 – initial samples; 1'-4' – used samples).

Absorption bands at 260, 325, 350 and 420 nm are observed for the initial Mn-SiO_2 (**Figure 4, a, curve 1**). The bands at 260 and 325 nm can be assigned to charge transfer transitions from oxygen ions to manganese ions in various valence and coordination states: to $O^{2-} \rightarrow Mn^{2+}$ transition and to $O^{2-} \rightarrow Mn^{3+}$, respectively [28]. The bands at 350 and 420 nm can be assigned to d-d transitions in Mn^{2+} ion – $^4T_{1g} \rightarrow {}^4A_{2g}$ [29] and $^6A_{1g} \rightarrow {}^4A_{1g}$ [28, 30], correspondingly. After catalytic reaction a noticeable reduction of the intensity of the bands in the region of 260 – 420 nm is observed and broad absorption bands in the region 450 – 800 nm appears (**Figure 4, a, curve 1′**). It indicates at increasing of amount of manganese in higher oxidation states. The bands at 450 – 550 nm are related to d-d transitions in manganese ions in different oxidation states [28, 30–31]. The band at 610 – 700 nm are likely to characterize the $^6A_{1g} \rightarrow {}^6T_{2g}$ [30] and $^6A_{1g} \rightarrow {}^6T_{1g}$ [32] transitions in Mn^{2+} ion, and the bands at 750 – 800 nm – the $^5B_{1g} \rightarrow {}^5A_{1g}$ transition in Mn^{3+} ion [28].

For the initial Mn-Al_2O_3 and Mn-ZSM-5 samples, wide bands centered at 500 and 550 nm, respectively, are observed (**Figure 4, a, curves 2, 3**). These bands are due to d-d tranisitons in Mn^{3+} and Mn^{4+} ions [30–31]. In this wavelength region an absorption band for the $^6A_{1g} \rightarrow {}^4T_{2g}$ transition in Mn^{2+} can also be found, but since d-d transitions in Mn^{2+} ion are both spin- and orbital-forbidden, this band would have a slight contribution. Weak bands at 260 and 360 nm responsible for Mn^{2+} ions are also present in the spectra of the initial Mn-Al_2O_3 and Mn-ZSM-5 (**Figure 4, a, curves 2, 3**). In the DR spectra of used Mn-Al_2O_3 and Mn-ZSM-5 samples absorption bands which can be assigned to Mn^{2+} (260, 360, 425 – 450 nm)

and Mn^{3+} (320, 500 nm) are observed (**Figure 4, a, curves 2′, 3′**).

Spectum of the initial Mn-ERI (**Figure 4, a, curve 4**) exhibits absorption in the region 270 – 500 nm which can be assigned to Mn^{2+} in MnO and remained without essential changes after catalytic reaction (**Figure 4, a, curve 4′**).

Since oxidative treatment is proved to be more favorable for CO oxidation catalysis than reductive treatment for all the studied catalysts previously treated at 350 ºC, the catalytic measurements were performed for 3%Mn-systems treated with air at 500 ºC also. It is found that this treatment lead to an increase of activity for Mn-ERI, Mn-ZSM-5 and Mn-Al_2O_3 catalysts in comparison with the samples treated at 350 ºC (**Table 1**). In the case of Mn-SiO_2 the treatment at 500 ºC results in activity decrease as compared to the sample treated at 350 ºC. Thus, activity in CO oxidation of the catalysts treated with air at 500 ºC follows in the order Mn-ZSM-5 > Mn-Al_2O_3 > Mn-SiO_2 > Mn-ERI (**Table 1**). This activity order differs from the activity order of the catalysts treated at 350 ºC, however Mn-ERI sample has the lowest activity irrespective of the temperature of previous treatment.

DR UV–Vis spectra of 3%Mn-systems treated at 500 ºC with air before and after catalysis are presented in **Figure 4, b**.

The spectra of the initial (**Figure 4, b, curve 1**) and used (**Figure 4, b, curve 1′**) Mn-SiO_2 contain absorption bands corresponding to Mn^{2+}, Mn^{3+}, Mn^{4+} ions. It should be noted, that according to the DR spectra of the the used Mn-SiO_2 systems both Mn^{2+} ions and Mn^{3+}/Mn^{4+} ions are found in the sample treated at 500 ºC, while Mn^{3+}/Mn^{4+} ions predominate in the sample treated at 350 ºC. It agrees with a higher catalytic activity of the Mn-SiO_2 sample treated at 350 ºC than at 500 ºC.

The DR spectra of the initial (**Figure 4, b, curve 2**) and used (**Figure 4, b, curve 2′**) Mn-Al_2O_3 system show presence of manganese predominantly in 3+ and 4+ oxidation states.

The DR spectra of Mn-ZSM-5 (**Figure 4, b, curves 3, 3′**) show absorption bands in all the range under study, intense absorption in the range 430 – 700 nm indicating at Mn^{3+} (and Mn^{4+}). Intesity of the band characterizing the $O^{2-} \rightarrow Mn^{2+}$ transition, noticeably decreases after the catalytic reaction, while intensity of the band for the $O^{2-} \rightarrow Mn^{3+}$ – increases. Thus, in the course of Mn-ZSM-5 development in the reaction mixture a further manganese oxidation up to the highest oxidation states (Mn^{+3}, Mn^{+4}) happens.

The DR spectra of the Mn-ERI sample treated at 500 ºC (**Figure 4, b, curves 4, 4′**) are similar to the spectra of the sample treated at 350 ºC (**Figure 4, a, curves 4, 4′**). However, intensity of the absorption bands above 370 nm for the Mn-ERI treated at 500 ºC somewhat increases after catalytic reaction, that indicates at slight presence of manganese in high valence states. It accords with higher activity of Mn-ERI

treated at 500 ºC as compared to activity of the sample treated at 350 ºC.

It is shown that in a result of the applied treatments the manganese ions in different oxidation states are formed in the case of Mn-catalysts on SiO_2, Al_2O_3, ZSM-5. Direct dependences of activities on surface areas aren't observed (**Table 2**).

Table 2. Specific surface area and pore volumes of supports and 3%Mn-systems (air, 350 °C)

Samples	S, m^2/g	*V*, cm^3/g
SiO_2	120	0.43
Al_2O_3	13	0.13
ZSM-5	245	0.08
ERI	220	0.14
3%Mn-SiO_2	100	0.05
3%Mn-Al_2O_3	12	0.07
3%Mn-ZSM-5	230	0.02
3%Mn-ERI	196	0.03

Mn-Al_2O_3 samples reveal average catalytic activities despite the least surface area and the biggest pore values of α-Al_2O_3 (i.e. boundary values of the textural parameters) among the applied supports. Mn-ZSM-5 samples reveal activities similar to Mn-Al_2O_3 in spite of less ZSM-5 pore diameter in comparison with Al_2O_3, that may indicates that mass transfer limitation doesn't occur in the course of catalytic reaction, and the activity is determined namely manganese state. Mn-ERI samples contain predominantly Mn^{2+} ions as active sites that causes the least catalytic activities of these samples. Reluctant formation of Mn^{3+}/Mn^{4+} may be associated with the narrowest pores (zeolite channels) in this support. Therefore, it is established that more active catalysts of CO oxidation contain manganese in different oxidation states (Mn^{2+}, Mn^{3+}, Mn^{4+}). And in the course of catalytic reaction a part of Mn^{2+} ions oxidized to higher oxidation states.

Conclusions

Consequently, MnO_x-containing catalysts supported on SiO_2, Al_2O_3 and zeolites ZSM-5, ERI were obtained by impregnation and an influence of previous treatment on their activity in CO oxidation was investigated. It was shown that activity of the catalysts after treatment at 350 °C, both reductive and oxidative, changed in the order Mn-ERI < Mn-ZSM-5 < Mn-Al_2O_3 < Mn-SiO_2. In the case of air treatment at 500 °C Mn-ZSM-5 and Mn-Al_2O_3 systems had the highest activities. The air treatment provided higher CO oxidation activity of the catalysts as compared with hydrogen-containing mixture treatment.

The study by temperature-programmed reduction with hydrogen showed that the greater amount of Mn cations of the highest reducibility in the catalysts, the higher their catalytic activity. Accords with DR UV–Vis spectroscopy, the Mn-catalysts contain non-stoichiometric oxide compounds with

manganese in different oxidation states (Mn^{2+}, Mn^{3+}, Mn^{4+}). It was established more active catalysts (Mn-SiO_2, Mn-Al_2O_3, Mn-ZSM-5) contain more manganese ions in higher oxidation states – Mn^{3+} and Mn^{4+}. This agrees with the fact of higher activity of the catalysts treated with air in comparison with those treated by H_2, since the latter contained lesser quantity of Mn^{3+} and/or Mn^{4+} species.

References

[1] F. Kapteijn, L. Singoredjo, A. Andreini, J.A. Moulijn, *Appl. Catal. B*, **1994**, 3, 173.

[2] Y. Peng, H. Chang, Y. Dai, J. Li, *Proc. Envir. Sci.*, **2013**, 18, 384–390.

[3] Zh. An, Y. Zhuo, *Chinese J. Catal.*, **2014**, 35, 120.

[4] J.W. Saalfrank, W.F. Maier, *Angew. Chem. Int. Ed*. **2004**, 43, 2028.

[5] S. Liang, F. Teng, G. Bulgan, R. Zong, Y. Zhu, *J. Phys. Chem. C.* **2008,** 112, 14, 5307.

[6] Y.-F. Han, F. Chen, Z. Zhong, K. Ramesh, L. Chen, E Widjaja, *J. Phys. Chem. B,* **2006,** 110, 48, 24450.

[7] R. Craciun, B. Nentwick, K. Hadjiivanov, H. Knözinger, *Appl. Catal. A.* **2003**, 243, 67.

[8] M.C. Álvarez-Galván, V.A. O'Shea de la Peña, J.L.G. Fierro, P.L. Arias. *Catal. Comm.* **2003,** 4, 223.

[9] G.S. Rozan, *J. Haz. Mat*., **2012**, 124, 221.

[10] K. Ramesh, L. Chen, F. Chen, Y. Liu, Z. Wang, Y.-F. Han, *Catal. Today.* **2008,** 131. 1-4, 477.

[11] L.-C. Wang, Q. Liu, X.-S. Huang, Y.-M. Liu, Y. Cao, K.-N. Fan, *Appl. Catal. B Envir.* **2009,** 88, 1-2, 204.

[12] O.V. Krylov, Heterogeneous Catalysis: Textbook, *M. PTC "Akademkniga"*, **2004**, 679 pp.

[13] Sh. Liang, F. Teng, G. Bulgan, R.Zong, Yo. Zhu, *J. Phys. Chem. C*, **2008**, 112, 14, 5307.

[14] M. Kantcheva, M.U. Kucukkal, S. Suzer, *J. Catal*. **2000**, 190, 144.

[15] J. Astudillo, G. Águila, F. Díaz, S. Guerrero, P. Araya, *Appl. Catal. A,* 2010, 381, 1–2, 169.

[16] M. Tepluchin, M. Casapu, A. Boubnov, H. Lichtenberg, D. Wang, S. Kureti. J.-D. Grunwaldt, *ChemCatChem*, **2014**, 6, 1763.

[17] J. Weitkamp, *Solid State Ionics*, **2000**, 131, 1-2, 175.

[18] Ch. Baerlocher, L.B. McCusker, D.H. Olson, Atlas of zeolite framework types (6th Ed.), 2007, *Elsevier*, 398 pp.

[19] E.M. Moroz, *Russ. J. Appl. Chem*., **1996**, 69, 11, 1584.

[20] L.P. Oleksenko, V.K. Yatsimirsky, G.M. Telbiz, L.V. Lutsenko, *Adsorp. Sci. Technol*.. **2004**, 22, 7, 535.

[21] V.K. Yatsimirskii, L.P. Oleksenko, L.V. Lutsenko, Yue Chen. *Russ. J. Phys. Chem.* **2008**, 82, 9, 1460.

[22] L.P. Oleksenko, L.V. Lutsenko, *Russ. J. Phys. Chem. A*, **2013**, 87, 2, 180.

[23] F. Arena, T. Torre, C. Raimondo, A. Parmaliana, *Phys. Chem. Chem. Phys.* **2001**, 3, 10, 1911.

[24] L. Singoredjo, R. Korver, F. Kapteijn, J. Moulijn, *Appl. Catal*. B. **1992**, 1, 4, 297.

[25] A. Derylo-Marczewska, W. Gac, N. Popivnyak, G. Zukocinski, S. Pasieczna, *Catal. Today*. **2006**, 114, 293.

[26] D.B. Akolekar, S.K. Bhargava, *App.Catal. A.* **207**, 355, 2001.

[27] K. Hadjiivanov, E. Ivanova, M. Kantcheva, *Catal. Comm*. **2002**, 3, 313.

[28] S. Velu, N. Shah, T.M. Jyothi, S. Sivasanker, *Micropor. Mesopor. Mater*. **1999**, 33, 1-3, 61.

[29] A.B.P. Lever. Inorganic Electronic Spectroscopy. Elsevier, Amsterdam, **1984**, 440.

[30] W. S. Kijlstra, E. K. Poels, A. Bliek, *J. Phys. Chem. B.* **1997**, 101, 3, 309.

[31] J.-Y. Wu, Sh.-H. Chien, B.-Z. Wan, *Ind. Eng. Chem. Res*. **2001**, 40, 1, 94.

[32] V.A. Shelke, S.M. Jadhav, S.G. Shankarwar, A.S. Munde, T.K. Chondhekar, *Bull. Chem. Soc. Ethiop*. **2011**, 25, 3, 381.